Electronic Supplementary Material (ESI) for Nanoscale.

Hierarchical PdNi alloy nanochains coupled with $Ni(OH)_2$ nanosheets to enhance the CO-poisoning resistance for methanol oxidation reaction

Anzhou Yang, ‡[ab] Keying Su, ‡[a] Yujia Liang,[a] Shan Yang,[a] Wu Lei,[b] Yawen Tang,*[a] and Xiaoyu Qiu*[a]

[a] *Jiangsu Key Laboratory of New Power Batteries, Jiangsu Collaborative Innovation Center of Biomedical Functional Materials, School of Chemistry and Materials Science, Nanjing Normal University, Nanjing 210023, P. R. China*

[b] *School of Chemical Engineering, Nanjing University of Science and Technology, Nanjing 210094, P. R. China*

Experimental Section

Reagents and Chemicals

Potassium tetrachloroplatinate (II) (K_2PdCl_4) were purchased from Shanghai D&B biological Sci-Tech Co., Ltd. (Shanghai, China). Potassium tetracyanonicolate ($K_2[Ni(CN)_4]$) was obtained from the Alfa Aesar chemical Co., Ltd (Shanghai, China). Poly (diallyl dimethyl ammonium chloride) (PDDA, *Mw*: 200,000-350,000), borane-tert-butylamine complex ($C_4H_{14}BN$) and commercial Pd black were purchased from Aladdin industrial corporation. (Shanghai, China). All chemicals used in this study were of analytical reagent (AR) without any further purification.

Synthesis of PdNi nanochains@$Ni(OH)_2$ nanosheets (PdNi NCs@$Ni(OH)_2$ NSs)

Typically, 1 mL of K_2PdCl_4 (0.05 M), 2 mL of PDDA (0.25 M) and 1 mL of $K_2[Ni(CN)_4]$ (0.05 M) were successively added to 5 mL of deionized water under magnetic stirring. Afterwards, 1 mL of $C_4H_{14}BN$ solution (5 mg mL^{-1}) was dropwise added into above solution. The mixture was stirred under room temperature for 1 h, and then underwent centrifugation at 18000 rpm for 8 min, washed with deionized water, and dried at 45 °C for 8 h in a vacuum dryer to collect the final products.

Characterizations

The morphology of PdNi NCs@$Ni(OH)_2$ NSs were firstly examined by high-resolution (HR) transmission electron microscopy (TEM) pictures (JEOL JEM-2100F, operated at 200 kV) and scanning electron microscopy (SEM) image (Hitachi S-4800, operated at 5 kV voltage). The components were tested by Energy Dispersive X-ray (EDX) measurements (JEOL JSM-7600F-type). UV-vis spectra were recorded on a Shimadzu UV3600 spectrophotometer equipped with an optical path length of 1 cm at room temperature. X-Ray Diffraction (XRD) patterns were carried out on Model D/max-rC X-ray diffractometer operated at 40 kV and 100 mA by using Cu Kα radiation source (λ= 1.5406 Å). High-resolution X-ray photoelectron spectroscopy (XPS) data were carried out on a Thermo VG Scientific ESCALAB 250 spectrometer with an Al Kα radiator and the binding energy was calibrated by means of the C 1s peak energy of 284.6 eV. XPS data were analyzed using XPS PEAK 4 software, and the binding energy was calibrated by means of the C 1s peak energy of 284.6 eV. The N_2

adsorption/desorption isotherms were measured at 77 K using a Micromeritics ASAP 2050 system. The specific surface area was calculated by Brunauer-Emmett-Teller method. The pore size distribution was determined using quenched solid density functional theory model for slit shaped and cylindrical pores.

Electrochemical measurements

All electrochemical measurements were carried out on a CHI 760E electrochemical analyzer (CH Instruments, Inc., Shanghai, China) at 25 °C. A conventional three-electrode cell was used, including a saturated calomel electrode (SCE) as the reference electrode, a graphite rod as the auxiliary electrode, and a catalyst-modified glassy carbon electrode as the working electrode. The catalyst ink was prepared by ultrasonically dispersing the mixture of 4 mg of catalyst, 0.8 mL of alcohol and 1.2 mL of deionized water. Then 5 μL of the catalyst ink was dropped onto the clean surface of glassy carbon electrode. After drying, the modified electrode was covered with 2 μL of Nafion solution (5 *wt*%) and dried again. The MOR performance of catalysts were evaluated in N_2-saturated 1 M KOH with or without 0.5 M CH_3OH solution at a scan rate of 50 mV s^{-1}. ECSA were calculated by the following formula:

$$ECSA = \frac{Q}{0.402\ mC\ cm^{-2} * m_{Pd}}$$

The MOR stability of PdNi NCs@$Ni(OH)_2$ NSs was examined by using chronoamperometry technique at a fixed potential of -0.2 V. The onset potential (E_{onset}) was measured by making a point of intersection, where the tangent of the reduction peak intersected with the horizontal line of zero current. CO stripping experiments were conducted in 1 M KOH. The electrolyte was first bubbled with 10% CO/N_2 while holding the working electrode at 1.0 V for 30 min. Then the solution was purged by flowing N_2 for 30 min to dislodge residual CO. Finally, the CV cycles were carried out from -0.8 to 0.2 V at 50 mV s^{-1} to record the CO stripping voltammetry.

Figures

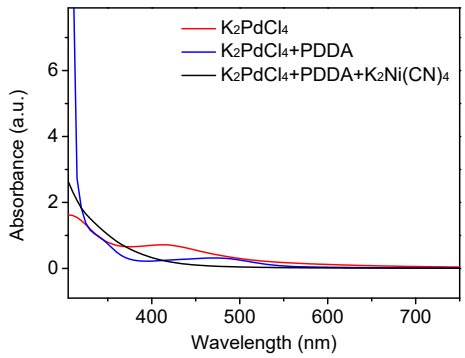

Fig. S1 UV-vis spectra of K_2PdCl_4 solution, K_2PdCl_4 + PDDA solution, and K_2PdCl_4 + PDDA + $K_2[Ni(CN)_4]$ solution.

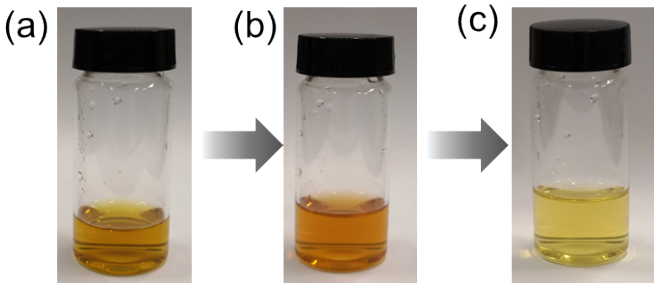

Fig. S2 (a) Photos of K_2PdCl_4 solution, (b) K_2PdCl_4 +PDDA solution, and (c) K_2PdCl_4 + PDDA + $K_2[Ni(CN)_4]$ solution

Fig. S3 Photograph of the PdNi cyanogels.

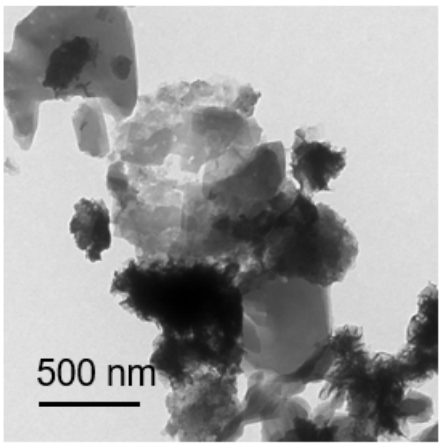

Fig. S4 Products obtained without adding PDDA.

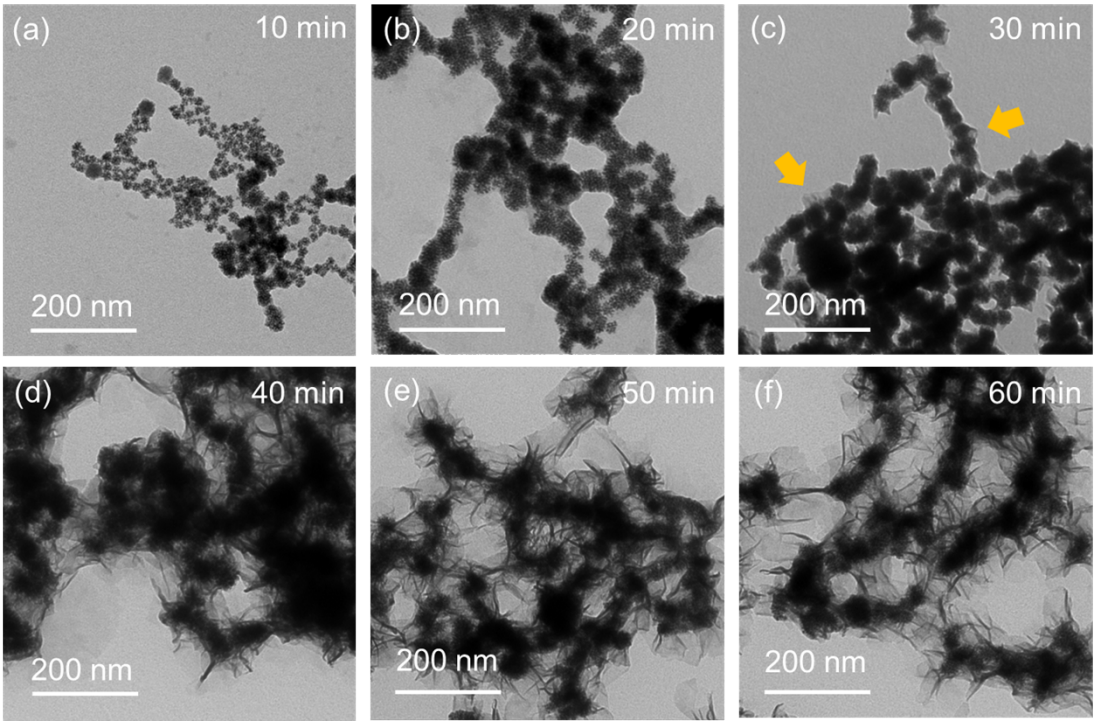

Fig. S5 Typical TEM images of intermediates collected at different reaction intervals. (a) 10 min, (b) 20 min, (c) 30 min, (d) 40 min, (e) 50 min, and (d) 60 min.

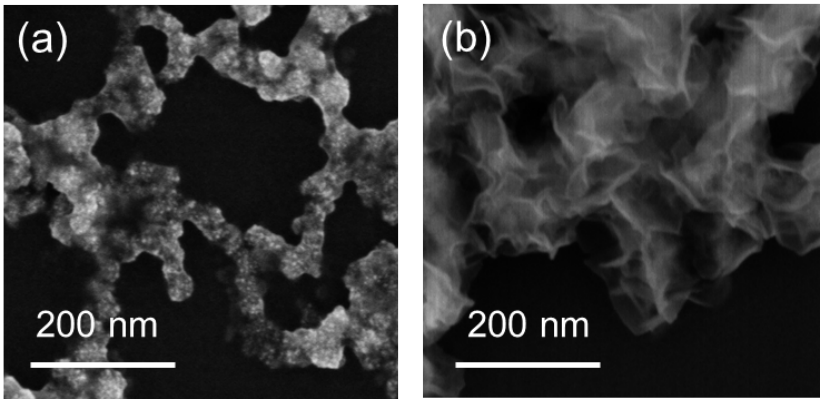

Fig. S6 SEM images of the (a) PdNi NCs and (b) PdNi NCs@$Ni(OH)_2$ NSs.

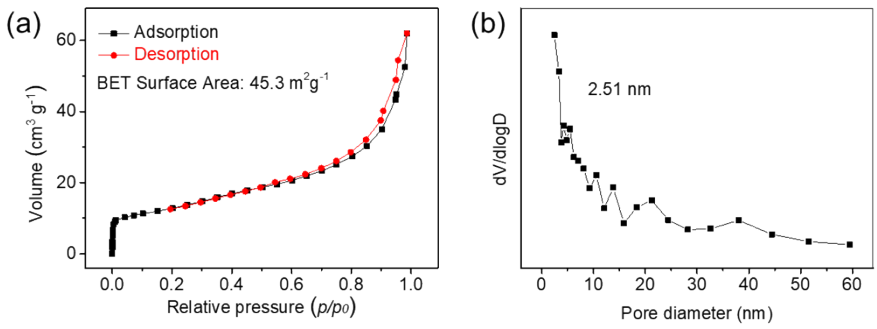

Fig. S7 (a) N_2 adsorption-desorption isotherms and (b) meso-pore size distribution of the PdNi NCs.

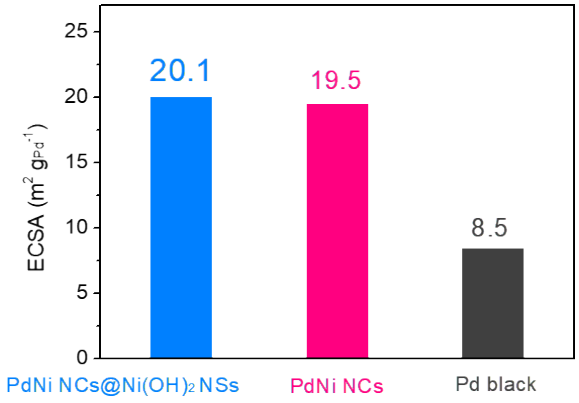

Fig. S8 ECSA histogram of PdNi NCs@$Ni(OH)_2$ NSs, PdNi NCs and Pd black.

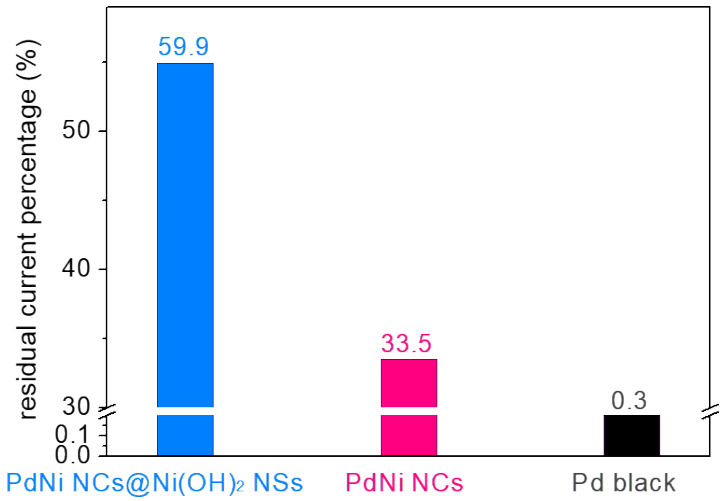

Fig. S9 Comparison of the stability of PdNi NCs@$Ni(OH)_2$ NSs and controllable samples.

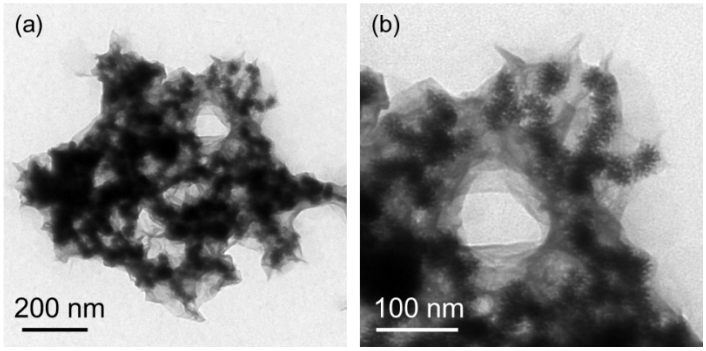

Fig. S10 TEM images of the PdNi NCs@$Ni(OH)_2$ NSs after chronoamperometry tests.

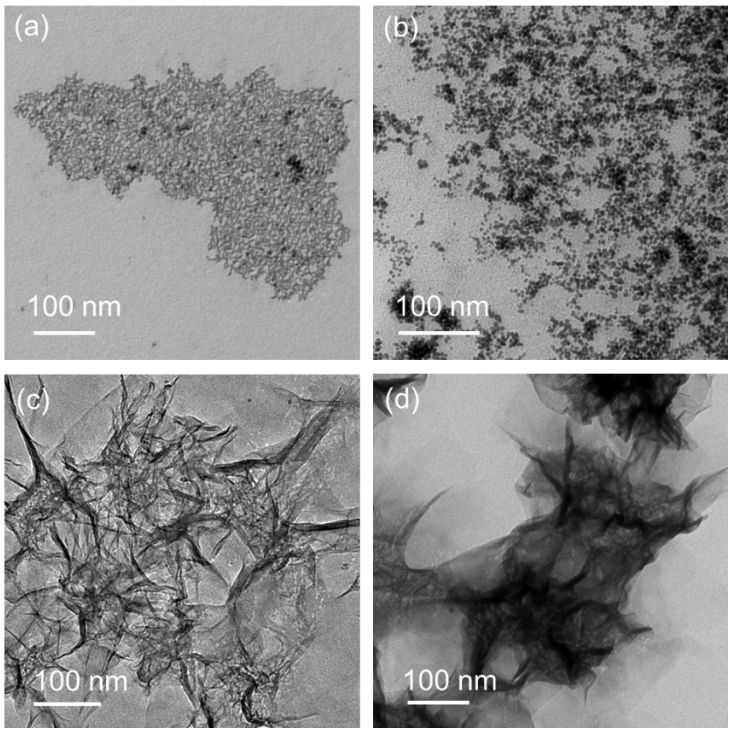

Fig. S11 TEM images of products prepared with (a) pure Pd^{2+} precursor, (b) Pd/Ni ratio of 4:1, (c) Pd/Ni ratio of 1:4, (d) pure $[Ni(CN)_4]^{2-}$ precursor.

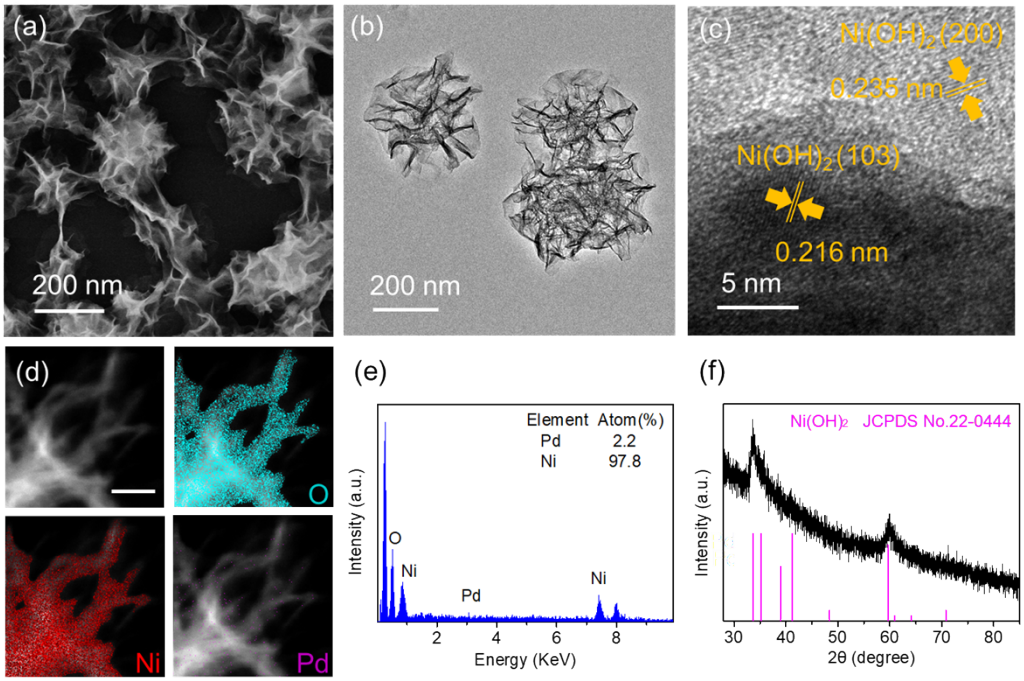

Fig. S12 (a) HADDF-STEM image, (b-c) HRTEM images, (d) elemental mapping images, (e) EDX spectrum, and (f) XRD pattern of $Ni(OH)_2$ NFs.

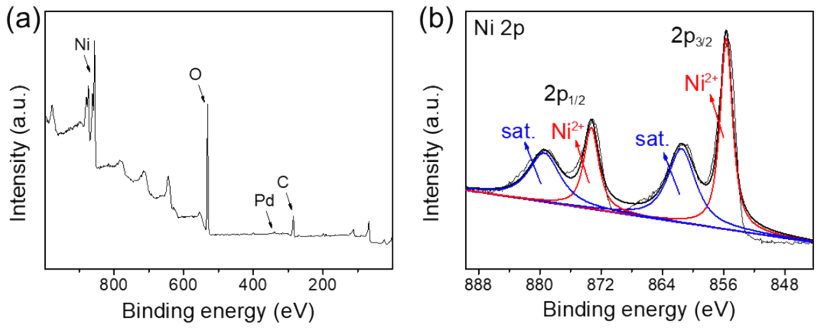

Fig. S13 (a) Full XPS survey of $Ni(OH)_2$ NFs. (b) High-resolution XPS survey at Ni 2p region.